

## ANALYSIS OF SHALLOW HEAT FLOW MEASUREMENTS ON MATTHEWS AND HUNTER VOLCANOES (SW PACIFIC)

ALAIN TABBAGH\* and MICHEL LARDY†

\**Département de Géophysique Appliquée, Université Paris 6, et Centre de Recherches Géophysiques, C.N.R.S., Garchy 58150, France; and* †*O.R.S.T.O.M., B.P. 5, Noumea cedex, Nouvelle Calédonie*

(Received March 1991; accepted for publication October 1992)

**Abstract**—Temperature measurements on shallow vertical profiles undertaken on Matthews and Hunter volcanoes of the New Hebrides arc (SW Pacific) demonstrate the absence of both unsteady and steady conductive abnormal flux at the location of the studied profiles. The reasons for this absence are explained in terms of limits in depth or magnitude for possible sources of heat inside the volcanoes. It implies that the magma chamber is of rather limited extent. This type of flux measurement has a low cost and it will be possible to implant a series of such temperature profiles on an edifice in order to obtain a map of the flux that could be widely used for the location of heat sources.

### NOMENCLATURE

$t$	time	$e$	thickness of a sill
$\tau$	time lag	$Q$	intensity of a source of heat (in joules)
$k$	thermal conductivity ( $\text{W m}^{-1} \text{K}^{-1}$ )	$\phi_z$	vertical flux of heat (deduced from theoretical calculations)
$\Gamma$	thermal diffusivity ( $\text{m}^2 \text{s}^{-1}$ )	$q$	experimental flux of heat ( $\text{W m}^{-2}$ )
$C_v$	volumetric heat capacity ( $\text{J m}^{-3} \text{K}^{-1}$ )	$\sigma$	fictitious surface charge density of heat ( $\text{W m}^{-2}$ )
$z$	vertical distance	$\vartheta$	temperature change generated by the presence of sources of heat
$r$	radial distance		
$h$	depth of a point below the ground surface		
$a$	radius (of a cylinder or of a sphere)		

### INTRODUCTION

Matthews and Hunter are the two southernmost active volcanoes of the Quaternary volcanic chain of the New Hebrides arc (Figs 1, 2). This arc corresponds to an intra-oceanic subduction zone. The petrographic and geochemical composition of both volcanoes are very similar, consisting of acid andesites containing a variety of inclusions (Maillet *et al.*, 1986): pyroxene and gabbroic cumulates, and doleritic cognate inclusions. The lava type and the evidence of recent pelean activity (Priam, 1964) show that they belong to the class of potentially dangerous active volcanoes. As no one lives on the island, they do not constitute a threat but it is always interesting to monitor their activity. They also provide a good experimental context for testing new sensors and measurement techniques. An experiment of remote monitoring using the Argos system was undertaken from September 1986 on the Matthews volcano (Lardy and Monzier, 1986) and from October 1988 on the Hunter volcano (Lardy *et al.*, 1988). Among other parameters, soil temperature was measured at several points along a shallow vertical profile. If such a profile is not located in an area of rapid fluid circulation, the data cannot be used for short-term volcanic activity forecasts. However, the data can be used to calculate the conductive heat flux and to obtain valuable information on the energy release by the volcano and on its internal structure. Whereas the temperature at any point at shallow depth is dependent on very local conditions, the heat flux, integrated over a sufficiently long period (one or more years), can reflect the existence of internal sources.



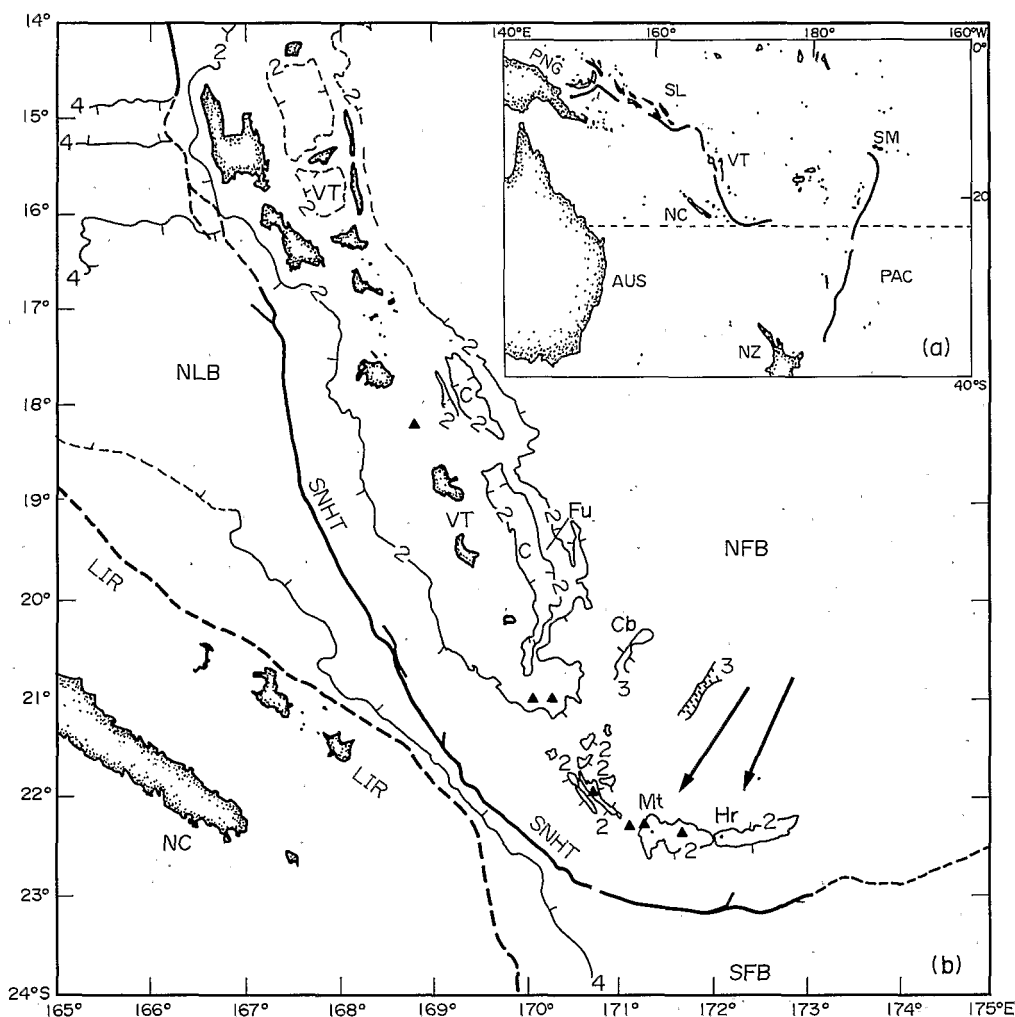


Fig. 1. Map of the southwestern Pacific (a) and outline of the Vanuatu–New Caledonia region (Maillet *et al.*, 1986). The location of Matheus and Hunter volcanoes is indicated by arrows. In (a) PAC = Pacific Ocean, AUS = Australia, NZ = New Zealand, NC = New Caledonia, PNG = Papua New Guinea, SL = Solomon Islands, VT = Vanuatu and SM = Samoa Islands. In (b) SNHT = Southern New Hebrides Trench, NFB = North Fiji Basin, NLB = North Loyalty Basin and LIR = Loyalty Islands Ridge. Numbers 2 and 4 indicate the depth of the sea in km.

The aim of this paper is to present the heat flux values obtained on the Matheus volcano at one point for the period October 1986–September 1988, and those obtained on the Hunter for the period October 1988–September 1989, in order to infer the location and extent of sources of heat inside the volcano. A map of the flux would have been preferable, but for this first experiment we were limited to only one profile on each volcano.

#### DETERMINATION OF THE HEAT FLUX FROM TEMPERATURE MEASUREMENTS

Considering a vertical profile constituted by  $n$  points of temperature measurement ( $n$  usually being between 2 and 6) at shallow depth (usually between 0.1 and 2 m) there are several methods

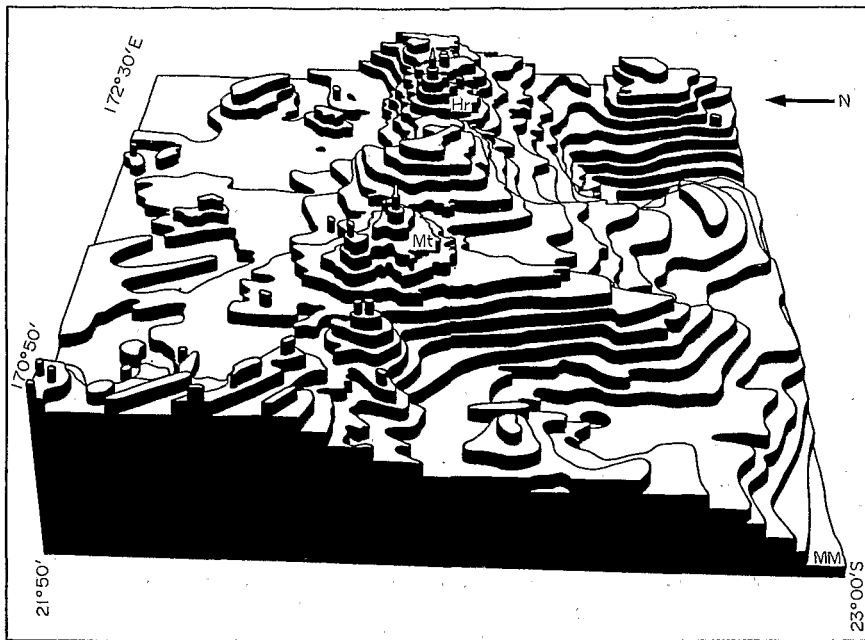


Fig. 2. 3-D bathymetry of Matthews and Hunter area (by Monzier using the data supplied by ORSTOM).  
Mt = Matthews; Hr = Hunter.

of determining the heat flux (Périsset and Tabbagh, 1981). All require knowledge of the thermal properties of the soil. In the experiment the temperature data are radio-transmitted and picked up by the satellite-borne Argos system. The rate of acquisition depends on the number of passes of the satellite in view of the transmitting station; at low latitude with two satellites there are eight or nine passes every 24 h. On a volcano both the unsteady (transient and sinusoidal) and the steady components of the heat flux must be considered (Tabbagh and Trézéguet, 1987). The unsteady component can originate either in the climatic conditions or in the internal activity of the volcano; the steady component (of time constant longer than 1 yr) accounts for the regional geothermal flux, the effect of heat sources (magma) inside or below the edifice and the long-term climatic changes; the term "base flux" would probably be better and will be used in this text.

Two methods can be considered for calculating the unsteady component:

(1) a numerical finite element method in which the vertical profile is divided into a series of elements, each element being limited by two temperature measurement points (Tabbagh and Trézéguet, 1987). This method requires more than three points in a profile;

(2) an analytical method, in which the flux variation is broken into a series of Heaviside functions whose amplitude,  $\Delta q_i$ , is determined from the temperature variation,  $\Delta \vartheta_i$ , at the considered time step and from the values of the preceding  $\Delta q_j$  amplitudes. Because there are two unknowns (external and internal flux sources) this method applies to profiles having two measurement points. If there are several points considered along a vertical profile, the least squares method is used to take advantage of all the points (Tabbagh and Trézéguet, 1987).

For calculating the steady component, the flux obtained at the lower element boundary in the finite element method can be averaged; in this case one has to consider a time series of one or several complete annual cycles. An analytical method can also be used to determine the steady temperature gradient between two different depths, by considering the temperature as the sum

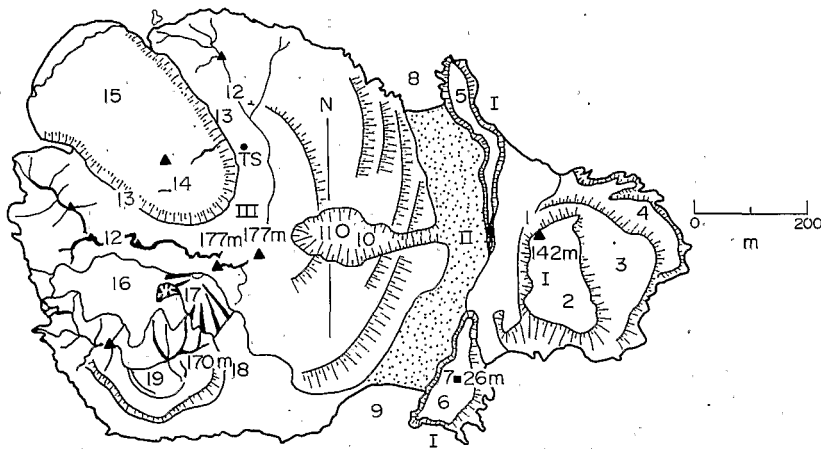


Fig. 3. Map of the Matthews volcano (Maillet *et al.*, 1986): I east-Matthews, II isthmus, III west-Matthews; 1 eastern peak; 2, 3 and 4 upper, middle and lower lava flow; 5 and 6 northern and southern basal scrap; 7 meteorological station; 8 and 9 northern and southern bay; 10 radial gorge; 11 lateral vent; 12 U-shaped central crater rim; 13 U-shaped gorge and T.S. point (where soil temperature measurements are recorded); 14 central crater; 15 NW-trending lava flow; 16 main volcanic graben; 17 youngest lateral vents; 18 volcanic graben; 19 southern peak.

of an annual sine variation and of a constant term and by searching for the best fit (in the least squares meaning) with actual data. This calculation applies even if the time series is shorter than the annual cycle.

## DESCRIPTION OF THE SITE AND HEAT FLUX MEASUREMENTS

### *Matthews volcano*

The map of this volcano is shown in Fig. 3. The temperature profile was located at the T.S. point 100 m above sea level (T.S. corresponds to the location of soil temperature measurements) on the inner side of the rim surrounding the north-west lava flow, where the sandy soil permits the installation of the sensors, and far from any fumarolic activity. Temperature measurements were made with copper wire thermistors at four depths: 3, 30, 60 and 120 cm. They were installed by excavating the earth, driving the sensor into the wall of the hole at each chosen depth (in such a manner that the distance from the hole wall is sufficient to avoid any influence of the thermal perturbation induced by the hole) and then refilling the hole with the same material (Lardy and Monzier, 1986). The western part of the volcano is the younger part, and probably formed in 1945 (Blot, 1976). Two annual cycles were recorded and studied here: October 1986–September 1987 and October 1987–September 1988.

*Thermal properties of the soil.* The calculation of heat flux requires a knowledge of the thermal and hydrodynamic parameters for the given profile: fluid characteristics in the case of forced convection (volumetric flow rate and volumetric heat capacity of the fluid) diffusivity and conductivity for heat conduction (volumetric heat capacity of the soil and thermal inertia can be easily deduced). As there is no convection (see below) only the last two properties have to be determined. The best solution is to perform *in situ* measurements with an active method (Tabbagh, 1985) and to check these by calculating the diffusivity from the damping or the phase lag with depth of the temperature variations. Unfortunately, no thermal property measurement apparatus was available when installing the sensors at the site. A sample was taken for later measurements in the laboratory using the active method. Because the exact porosity and

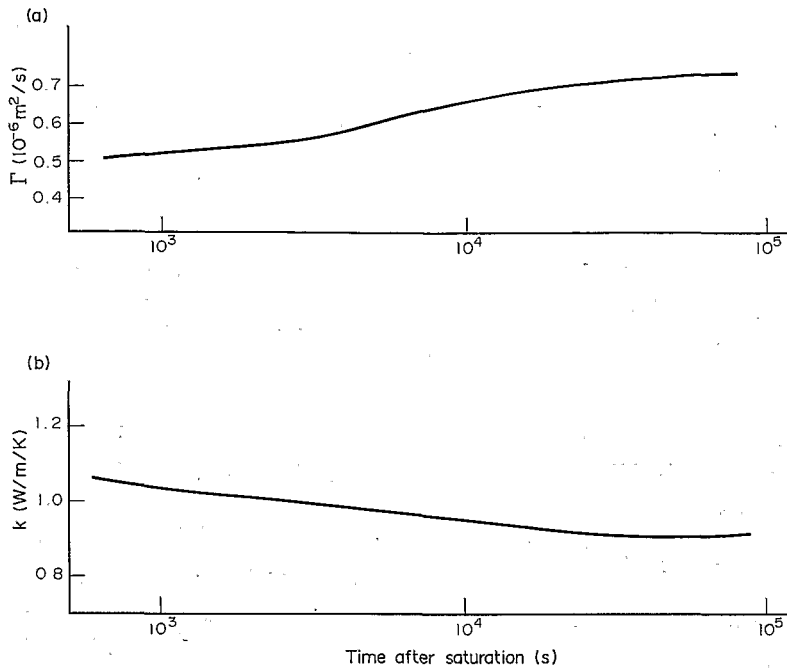


Fig. 4. Time variation of the thermal properties of a soil sample from Matthews volcano after compaction and saturation (laboratory measurements): (a) diffusivity; (b) conductivity.

moisture content were unknown, a first measurement was performed on the sample, giving a small conductivity ( $k = 0.63 \text{ W m}^{-1} \text{ K}^{-1}$ ) and a high diffusivity ( $\Gamma = 0.76 \times 10^{-6} \text{ m}^2 \text{ s}^{-1}$ ). The soil was then compacted and saturated with water, and the evolution with time of both properties was monitored while the soil was drained of water (Fig. 4). Owing to the coarse composition of this soil, it is reasonable to consider that the soil is well drained and not saturated *in situ* and that the most likely values of its properties are  $k = 0.92 \text{ W m}^{-1} \text{ K}^{-1}$  and  $\Gamma = 0.7 \times 10^{-6} \text{ m}^2 \text{ s}^{-1}$ .

Thermal diffusivity only can be determined from temperature records; this was done month by month from the damping of the modulus of the diurnal temperature variation. The medians obtained were:

- (1)  $0.42 \times 10^{-6} \text{ m}^2 \text{ s}^{-1}$  between 3 and 30 cm, with an interquartile distance of  $0.044 \times 10^{-6} \text{ m}^2 \text{ s}^{-1}$ ; and
- (2)  $0.55 \times 10^{-6} \text{ m}^2 \text{ s}^{-1}$  between 3 and 60 cm, with an interquartile distance of  $0.03 \times 10^{-6} \text{ m}^2 \text{ s}^{-1}$ .

The values are quite scattered, showing an increase of diffusivity with depth (probably caused by decreasing porosity). The values obtained between 3 and 120 cm from the damping of the annual variation are  $0.50 \times 10^{-6} \text{ m}^2 \text{ s}^{-1}$  for cycle 1, and  $0.61 \times 10^{-6}$  for cycle 2. The change can probably be explained by moisture variations.

The discrepancy between the diffusivity values obtained from laboratory measurements and those obtained from the damping of temperature originates in the inhomogeneity of the soil *in situ*. The second values are more reliable, as they are more representative of the *in situ* temperature behaviour, but the first values represent a useful control. Values of  $0.50 \times 10^{-6} \text{ m}^2 \text{ s}^{-1}$  for diffusivity and  $0.9 \text{ W m}^{-1} \text{ K}^{-1}$  for conductivity were then adopted for the following calculations of heat flux, with an estimated error of 20%.

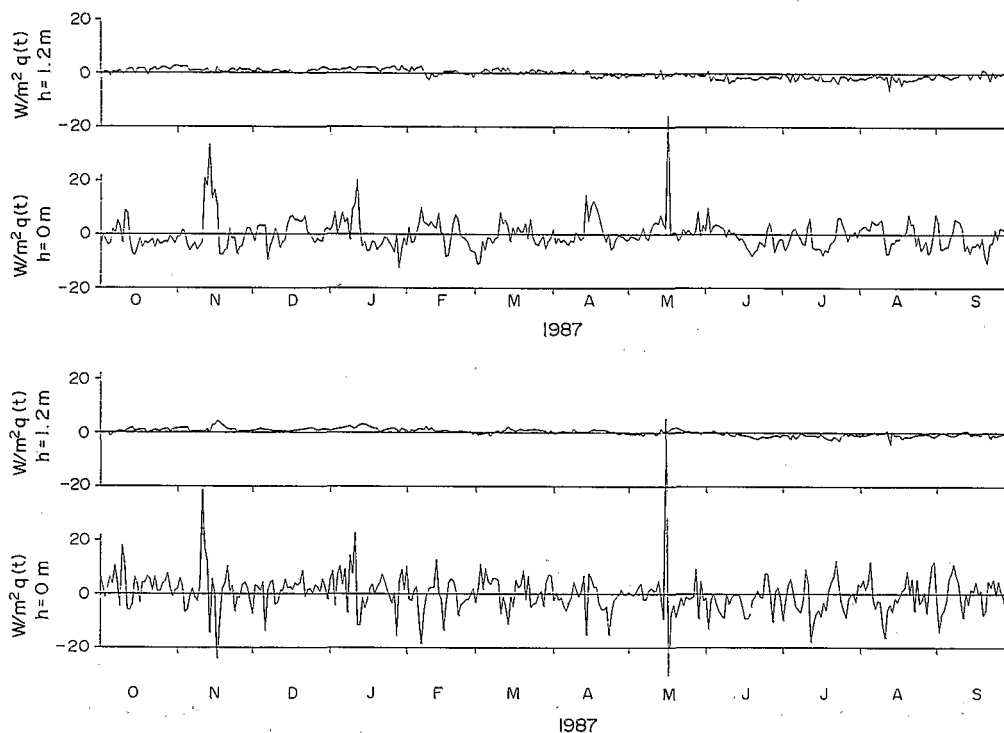


Fig. 5. Unsteady flux values,  $q(t)$ , at point T.S. on Matthews volcano for the first annual cycle. At the top, calculations by the finite element method; below, calculation by Heaviside's series decomposition. The spikes correspond to climatic events also observed on air temperature and atmospheric pressure;  $h$  corresponds to the depth where the flux is calculated.

*Data pre-processing.* The Argos transmission supplies six temperature values per day at each depth and it is difficult to filter out the diurnal variation by a simple averaging. To minimize the effect of shorter climatic events we took the average of the values measured during the second part of the night between 1.00 and 7.00 a.m. local time. The values for 3 cm are systematically lower than the correct diurnal mean value, so they have not been taken into account for the steady flux calculation.

*Unsteady heat flux.* The unsteady fluxes obtained for the first annual cycle are presented in Fig. 5 and those for the second cycle in Fig. 6 using both the analytical calculation and the finite element method. Flux variations are more important at the ground surface than at 1.2 m depth; in both cases there is a superimposition of annual and transient variations. There is no evidence of convective flux: the temperatures are "normal"; there are no fumaroles; when calculating the correlation function (normalized covariance) (Fig. 7) between the flux at 0 and 1.2 m a maximum for a 6 day time lag is apparent, which agrees very well with a conduction transfer. That type of transfer can be characterized by a value of the dimensionless parameter (similarity factor directly deduced from the diffusion equation)  $h^2/(4\Gamma\tau)$  not far from 1,  $\tau$  being the time lag,  $\Gamma$  the thermal diffusivity and  $h$  the depth; for the considered diffusivity its value is 1.4. The sign of  $\tau$  also indicates that at the considered point there was no transient flux of internal origin during the 2 yr of observations.

*Base flux.* The notion of base flux is not absolute, and corresponds to that component of the flux which did not vary during the observation time. It inevitably includes, in addition to the true

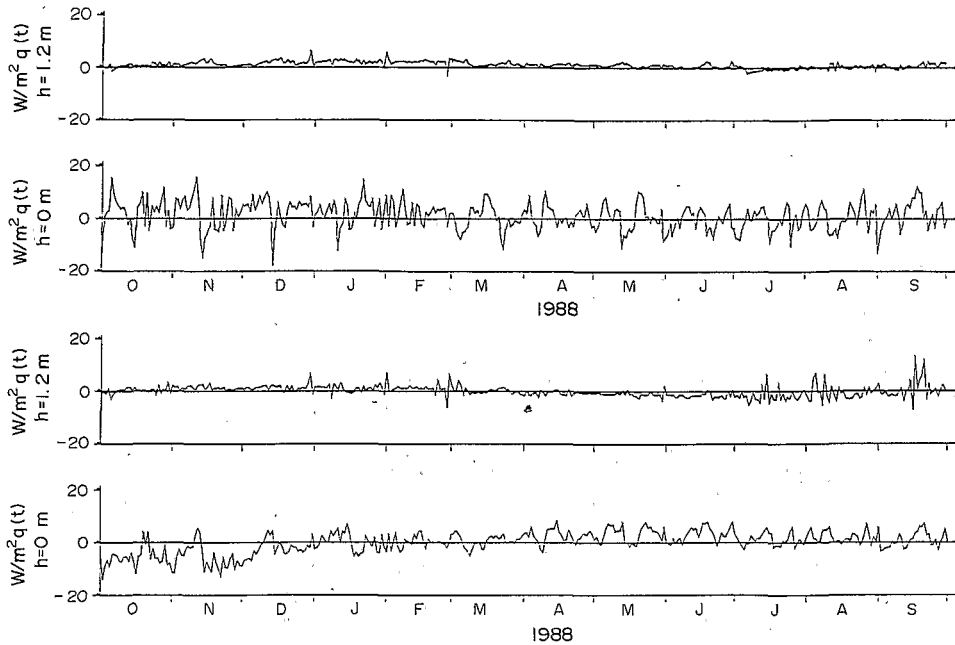


Fig. 6. Unsteady flux values,  $q(t)$ , at point T.S. on Matthews for the second annual cycle, calculated at depth  $h$ .

effect of internal sources, a component corresponding to slow climatic variations of longer than 1 yr. Because these variations are largely unknown, it is very often impossible to determine its value from shallow depth temperature records except in a high flux area (this can be the case on volcanoes) where the flux of internal origin is sufficiently higher than the long-term climatic noise (Tabbagh and Trézéguet, 1987). For the first annual cycle, and assuming a conductivity of  $1 \text{ W m}^{-1} \text{ K}^{-1}$ , one obtains the value of  $-0.033 \text{ W m}^{-2}$  using the finite element method at 1.2 m, and  $-0.029 \text{ W m}^{-2}$  by applying the heat conduction formula to the stationary temperature values between 0.6 and 1.2 m (the minus sign indicates that the flux is upward). In flux determinations the errors resulting from temperature measurements are negligible compared with those produced by conductivity uncertainty. For the second annual cycle, the corresponding values are  $0.002$  and  $0.008 \text{ W m}^{-2}$ , indicating downward flux. All the values are in the range of long-term climatic noise, and one can infer initially that there is no abnormal effect at point

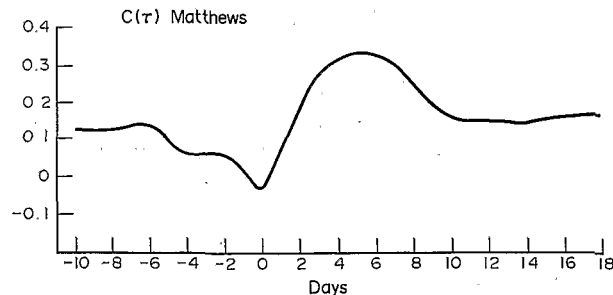


Fig. 7. Correlation function between the unsteady fluxes at  $h = 0$  and 1.2 m, for the first annual cycle at point T.S. on Matthews volcano. The correlation used here corresponds to the normalized covariance (dimensionless parameter).

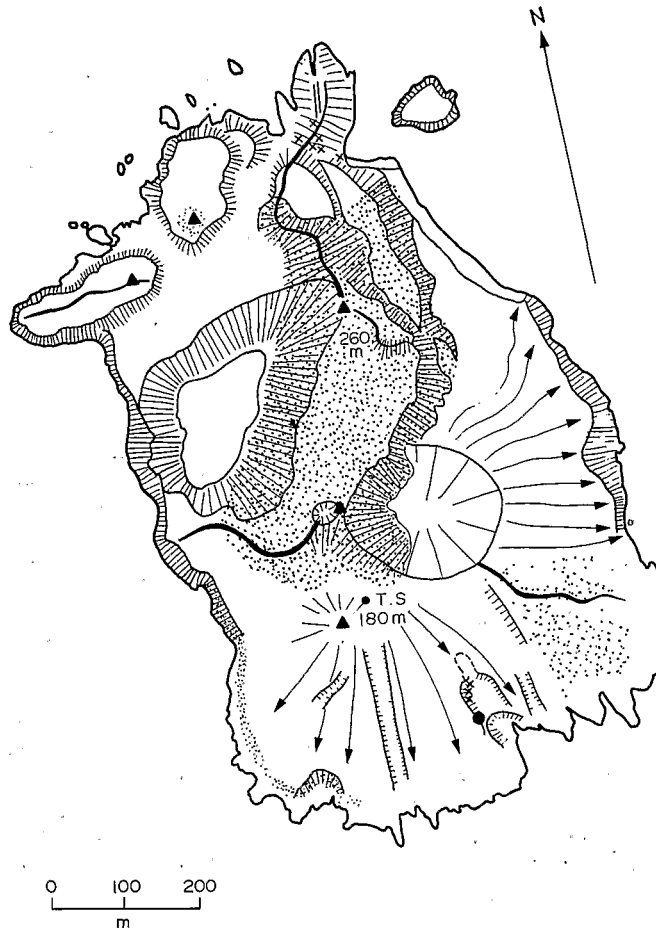


Fig. 8. Map of the Hunter volcano (Maillet *et al.*, 1986). T.S. corresponds to the location of soil temperature measurements.

T.S., which implies that the internal sources, if they exist, are too deep or too small to produce any measurable effect. This problem will be considered again later.

#### *Hunter volcano*

The soil temperature profile was installed in the saddle 50 m to the north of the southern summit (180 m) of the volcano (Fig. 8). The thermistors were placed at 30, 60, 90 and 120 cm using the same technique as that used on the Matthews (Lardy *et al.*, 1988). The first geological observations suggest that the main centre of activity shifted from the north (older) to the south (younger). The southern lava flow composed of acidic viscous lava looks very similar to the western one on Matthews. One annual cycle of data is available (October 1988–September 1989) but the 1.2 m sensor failed at the beginning and was repaired only during June 1989.

*Thermal properties of the soil.* As with Matthews, no direct measurements could be made *in situ* during the installation of the sensors and the same procedure was used in the laboratory. Four different samples were available corresponding to the different depths. Hunter's soil is mainly fine sand with only a few pebbles. This soil is very homogeneous and, after humidifica-

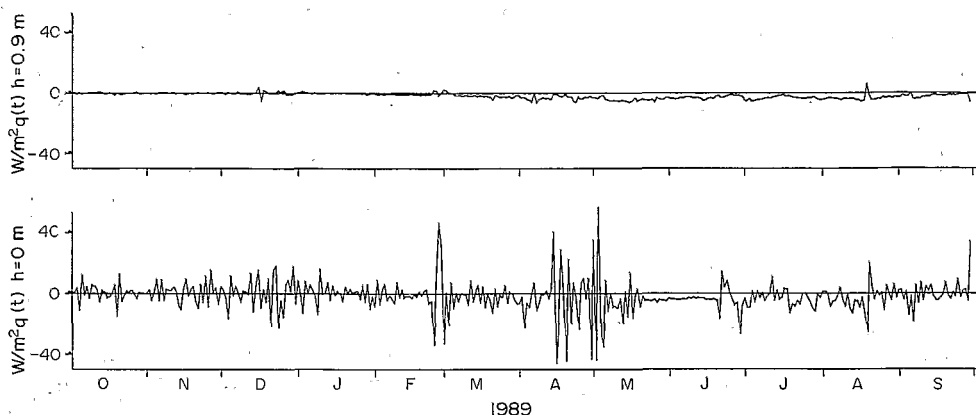


Fig. 9. Unsteady flux values at T.S. point on Hunter for the annual cycle.

tion and compaction, very stable values of  $\Gamma = 0.5 \times 10^{-6} \text{ m}^2 \text{ s}^{-1}$  and  $k = 1 \text{ W m}^{-1} \text{ K}^{-1}$  were obtained.

The diurnal temperature variation was difficult to use for diffusivity calculations because the upper sensor was at 30 cm depth where the damping of this variation is important; the median of the diffusivity values, however, calculated month by month from 30 and 60 cm deep temperature phase lags is equal to  $0.25 \times 10^{-6} \text{ m}^2 \text{ s}^{-1}$ . From the damping of the modulus of the annual temperature variation one again obtains  $0.25 \times 10^{-6} \text{ m}^2 \text{ s}^{-1}$  between 30 and 90 cm, which seems abnormally low. Owing to this discrepancy, two sets of values were used for flux calculations:  $0.25 \times 10^{-6} \text{ m}^2 \text{ s}^{-1}$  and  $0.6 \text{ W m}^{-1} \text{ K}^{-1}$  on the one hand, and  $0.50 \times 10^{-6} \text{ m}^2 \text{ s}^{-1}$  and  $1 \text{ W m}^{-1} \text{ K}^{-1}$  on the other (the first set corresponds to the values deduced from temperature damping, the second to laboratory measurements).

*Data pre-processing.* The procedure was the same as that applied to Matthews data, but errors in transmission or sensor breakdown generated wrong values that were eliminated and replaced by linearly interpolated ones. The 1.2 m depth measurements were not taken into account because the sensor failed during too long a period of the cycle. Thus only three points were used and the calculations are based only on analytical methods.

*Unsteady heat flux.* The results obtained at  $h = 0$  and 0.90 m are presented in Fig. 9. They show the same general aspect as those obtained on Matthews, but it should be noted that the flux value at  $h = 0$  m is less constrained because of the absence of temperature measurements at 3 cm. The correlation between fluxes at the two depths has the same aspect as in Fig. 7 for Matthews, with a maximum for a 3 day phase lag. A diffusivity value of  $0.50 \times 10^{-6} \text{ m}^2 \text{ s}^{-1}$  agrees better with this result than the  $0.25 \times 10^{-6}$  value. Again there is no transient of internal origin apparent at the considered point.

*Base heat flux.* An assumed conductivity of  $1 \text{ W m}^{-1} \text{ K}^{-1}$  gives, between 60 and 90 cm, a value of  $0.155 \text{ W m}^{-2}$ . If the conductivity is reduced to  $0.6 \text{ W m}^{-1} \text{ K}^{-1}$ , the flux will be reduced in the same proportions, but in no case would it give information on internal sources of heat.

## IMPLICATIONS OF THE RESULTS OBTAINED FOR THE STEADY FLUX

### *Comparison with climatological data*

Contrary to the results from Mount Etna (Tabbagh and Trézéguet, 1987), the base flux values

obtained at shallow depth on the two volcanoes do not show evident effects of internal sources of heat and seem likely to have originated in the long-term climatic variations. It would, therefore, be interesting to compare them with flux values obtained outside the volcanic context but in the same climatic environment. Unfortunately the data on the two volcanoes are not synchronous and could not be compared either directly or with the only other existing values acquired in Noumea (Nouvelle Calédonie) by J. P. Brun (personal communication) during the period March 1978–December 1980. These measurements were performed at five depths, 5, 10, 20, 50 and 100 cm, at a sampling rate of three per day (6, 12 and 18 h local time). There are no direct measurements of the soil thermal properties, but, from the damping of the modulus of the annual variation, a value of  $0.45 \times 10^{-6} \text{ m}^2 \text{ s}^{-1}$  was obtained for diffusivity, which most likely corresponds (due to the soil type and the moisture content) to a conductivity of  $1.2 \text{ W m}^{-1} \text{ K}^{-1}$ . As frequently occurs in climatological stations, the soil is covered by grass. Using the above conductivity value, the calculated steady flux is  $-0.141 \text{ W m}^{-2}$  for the duration of the whole experiment (1037 days),  $-0.128 \text{ W m}^{-2}$  for 1979 and  $-0.163 \text{ W m}^{-2}$  for 1980.

These values indicate the order of magnitude of the long-term climatic variations. Comparing with these values, one can conclude that the results obtained on both volcanoes are within this noise and that we have to consider that the base flux is null or near zero at each point. We thus have no positive conclusions, and have to interpret these negative conclusions. In particular, we can define the minimum distance and volume of several types of possible sources of heat that could produce the observed effects.

## SOURCES OF HEAT IN AN HOMOGENEOUS GROUND WITH HORIZONTAL SURFACE

### *Cooling of a neck*

Both the western flow on Matthews and the southern flow on Hunter are not far from the measuring point. The flows must have been fed by a pipe containing liquid lava during the phase of activity, and one can model this pipe by a simple vertical cylinder. The lava at Matthews was liquid about 45 yr ago, but we have no historical information on Hunter (Lardy *et al.*, 1988). Based on the chemical composition of the lava, however, its initial temperature,  $\vartheta_0$ , was  $1000^\circ\text{C}$  above the average value of the surroundings (roughly  $20^\circ\text{C}$ ).

The problem to be solved is presented in Fig. 10a. The neck is considered as equivalent to a line of instantaneous point sources of intensity  $Q = C_v \vartheta_0 \pi a^2 dz$  at time  $t = 0$  ( $a$  being the radius of the cylinder and  $C_v$  the volumetric heat capacity of the lava). Using the corresponding Green's function (Carslaw and Jaeger, 1959) and considering the image of each source to satisfy the limiting condition  $\vartheta = 0$  at the ground surface, one obtains:

$$\vartheta(r, z, t) = \vartheta_0 \pi a^2 \left\{ \int_0^\infty \frac{\exp(-((z-\xi)^2 + r^2)/(4\Gamma t))}{(4\pi\Gamma t)^{3/2}} d\xi - \int_{-\infty}^0 \frac{\exp(-((z+\xi)^2 + r^2)/(4\Gamma t))}{(4\pi\Gamma t)^{3/2}} d\xi \right\}$$

for temperature, and

$$\phi_z = -k \partial \vartheta / \partial z = -\frac{2k\pi a^2 \vartheta_0}{(4\pi\Gamma t)^{3/2}} \exp(-(z^2 + r^2)/4\Gamma t)$$

for heat flux. Adopting the following values for the variables corresponding to the case of Matthews:  $t = 1.42 \times 10^9$ ,  $\Gamma = 10^{-6} \text{ m}^2 \text{ s}^{-1}$ ,  $k = 2.5 \text{ W m}^{-1} \text{ K}^{-1}$  (for the whole volcano these

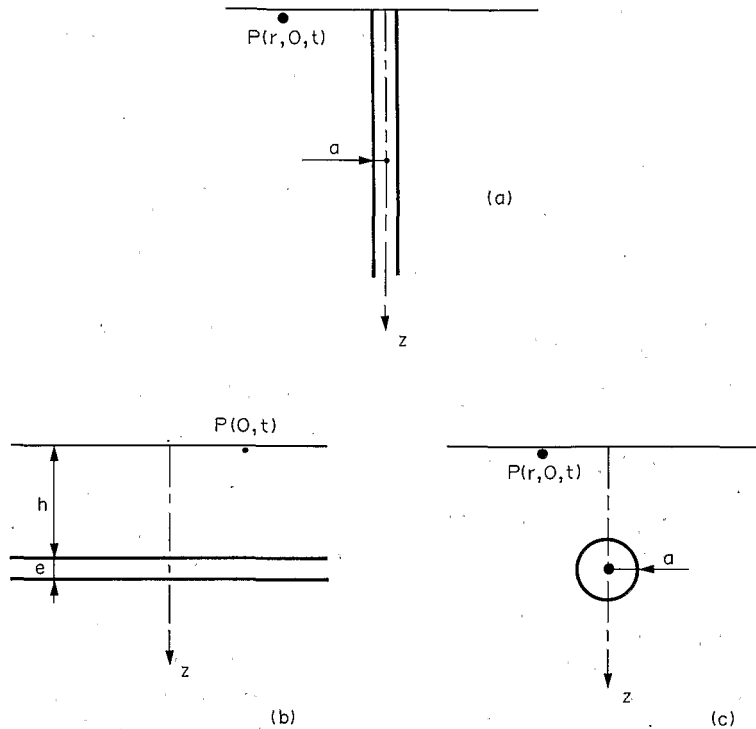


Fig. 10. Theoretical modelling for three different types of internal sources of heat: (a) neck; (b) sill; (c) spherical pocket or chamber. The flux is calculated at point P. The circle in (c) refers to the magma chamber of radius  $a$ .

values are preferable to that of soil),  $\vartheta_0 = 1000^\circ\text{C}$ ,  $z = 0$ ,  $r = 100$  m and  $a = 10$  m, one obtains  $\phi_z = -0.113$   $\text{W m}^{-2}$ . For Hunter, the order of magnitude of all the parameters would be equivalent. The absence of significant flux at the measurement points can easily be explained by the distance from the neck.

#### Cooling of a magma pocket

One has normally to consider a magma pocket inside or under an active volcano; two simple models can be used to evaluate the corresponding flux: a sill (Fig. 10b) or a spherical chamber (Fig. 10c). Adopting both models can lead to conclusions that are independent of the exact, and unknown, shape of the feature. In the first case one considers a planar instantaneous source of  $C_v\vartheta_0e$  intensity ( $e$  being the thickness of the sill) per square metre at  $t = 0$ , located at  $z = h$  depth. The temperature is given by the following expression:

$$\vartheta(z, t) = \vartheta_0 e \left\{ \frac{\exp(-(z-h)^2/4\Gamma t)}{(4\pi\Gamma t)^{1/2}} - \frac{\exp(-(z+h)^2/4\Gamma t)}{(4\pi\Gamma t)^{1/2}} \right\}$$

so that at  $z = 0$ ,

$$\phi_z(0, t) = \frac{-k\vartheta_0 e}{(4\pi\Gamma t)^{1/2}} \frac{h}{\Gamma t} \exp(-h^2/4\Gamma t).$$

Assuming, as in the preceding case, that  $t = 1.42 \times 10^9$  s,  $\Gamma = 10^{-6}$   $\text{m}^2 \text{s}^{-1}$ , and  $k = 2.5$   $\text{W m}^{-1} \text{K}^{-1}$ ,  $\vartheta_0 = 1000^\circ\text{C}$ , and  $e = 10$  m, one obtains the following numerical values:

$$\begin{aligned}
 \text{for } h = 60 \text{ m,} & \quad \phi = -4.2 \text{ W m}^{-2} \\
 h = 100 \text{ m,} & \quad \phi = -2.21 \text{ W m}^{-2} \\
 h = 150 \text{ m,} & \quad \phi = -0.379 \text{ W m}^{-2} \\
 h = 200 \text{ m,} & \quad \phi = -0.023 \text{ W m}^{-2}.
 \end{aligned}$$

For a spherical pocket, the flux expression derived from the temperature expression is (at  $r = 0$  and  $z = 0$ ):

$$\phi_z(0, t) = -k\vartheta_0 \frac{4a^3}{3\pi^{1/2}} \frac{4h}{(4\Gamma t)^{5/2}} \exp(-h^2/4\Gamma t).$$

Using the same numerical values, one obtains:

$$\begin{aligned}
 \text{for } h = 100 \text{ m and } a = 10 \text{ m,} & \quad \phi = -0.052 \text{ W m}^{-2} \\
 h = 100 \text{ m and } a = 50 \text{ m,} & \quad \phi = -6.6 \text{ W m}^{-2} \\
 h = 200 \text{ m and } a = 50 \text{ m,} & \quad \phi = -0.067 \text{ W m}^{-2}.
 \end{aligned}$$

It is then likely that a pocket that has just fed a recent flow does not give an observable flux at the ground surface if, for instance,  $h$  is greater than 200 m.

#### *Effect of a magmatic chamber*

The preceding calculations show that the feeding of a recent lava flow is unlikely to produce the heat flux observable at the ground surface. This is in part the result of the short time lapse since the last eruption and in part of the too small volume or too great depth of these sources of heat. For the numerical value adopted for  $t$ , the quantity  $h^2/4\Gamma t$  is equal to 1 when  $h = 75$  m. But we have also to consider the case of a magma chamber in place for a long time. Given a spherical chamber of radius  $a$  centred at depth  $h$ , the steady vertical heat flux is given by the expression:

$$\phi_z = k\vartheta_0 a \left\{ \frac{z-h}{(r^2 + (z-h)^2)^{3/2}} - \frac{z+h}{(r^2 + (z+h)^2)^{3/2}} \right\}.$$

Thus at  $r = 0$  and  $z = 0$ ,

$$\phi_z = -\frac{2k\vartheta_0 a}{h^2}.$$

Assuming  $k = 2.5 \text{ W m}^{-1} \text{ K}^{-1}$  and  $\vartheta_0 = 1000^\circ\text{C}$ , one has:

$$\begin{aligned}
 \text{for } h = 500 \text{ m and } a = 50 \text{ m,} & \quad \phi_z = -1.00 \text{ W m}^{-2} \\
 h = 1000 \text{ m and } a = 100 \text{ m,} & \quad \phi_z = -0.49 \text{ W m}^{-2} \\
 h = 1000 \text{ m and } a = 50 \text{ m,} & \quad \phi_z = -0.25 \text{ W m}^{-2} \\
 h = 2000 \text{ m and } a = 200 \text{ m,} & \quad \phi_z = -0.13 \text{ W m}^{-2}.
 \end{aligned}$$

Thus a depth of 2 km is sufficient, for a relatively small magma chamber, to explain the negligible surface flux. This depth corresponds to the base of the submarine cone of Matthews.

#### *Effect of the general shape of the volcano*

In the preceding calculations the ground is assumed to have a horizontal surface. This approximation is reasonable for shallow sources, neck or magma pockets, at a depth of 100 or 200 m, but less adequate for the calculation of the effect of a magmatic chamber where the

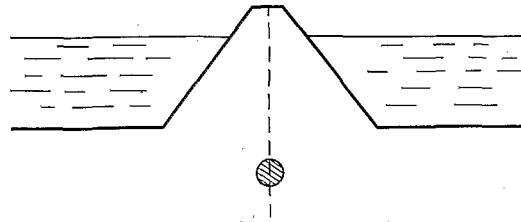


Fig. 11. Modelling for the calculation of the influence of the shape of the volcano when the flux is generated by a magma chamber. The dashed line corresponds to the axis symmetry, the circle to the magma chamber and the bold line to the volcano and sea floor.

general conical shape of the volcano may introduce a reduction of the surface steady flux of heat. We then consider the model presented in Fig. 11.

Because the problem is a 3-D one (2-D if the chamber is centred on the axis of symmetry) the calculations are more cumbersome and a numerical method has to be used. Considering the parallelism that exists between the steady temperature distribution and electric potential distribution in electrical prospecting, we chose to use the method first proposed by Alfano (1959) and to consider the discontinuity between the ground and the sea, or the air, as equivalent to a distribution of heat sources located on it. In this case the condition  $\vartheta = 0$  has to be verified, because the sea or the air have the ability to absorb any amount of heat; considering the fictitious charge density,  $\sigma$ , this condition is equivalent to  $\partial\vartheta/\partial n = 4\pi\sigma(r)$ , at any point  $r$ , on the discontinuity. The temperature of the ground,  $\vartheta$ , is the sum of the effect of each surface charge and of the source of heat corresponding to the magma chamber. By discretizing the surface into ring facets of constant charge density, and by writing the above equation for each facet, one gets a system of linear equations that can be solved to obtain the values of the charge density and then to calculate the flux and the temperature everywhere in the ground.

We consider the same numerical values as in the preceding examples,  $a = 50$  m,  $k = 2.5$  W  $m^{-1}$   $K^{-1}$ ,  $\vartheta_0 = 1000^\circ C$  (which corresponds to a heat source of 1.6 MW), and a cone of  $70^\circ$  half-angle with its top at 2000 m above the sea floor. For a magma chamber centred 100 m below the sea floor, the vertical flux differs from that of a flat homogeneous ground; as shown in Fig. 12, the difference is small at depth, less than 1% at sea floor level, but increases as the

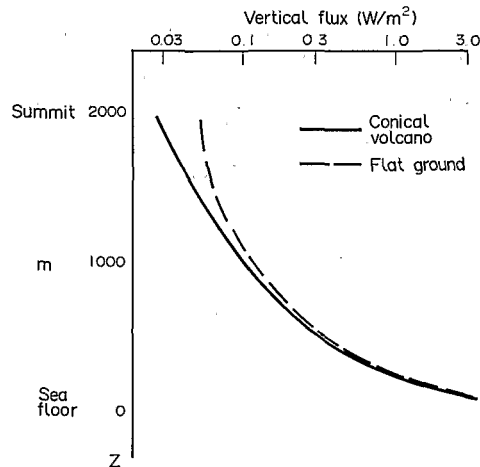


Fig. 12. Flux variation at the vertical axis of the chamber, for a flat ground and a conical volcano.

measurement point approaches the surface to reach a 50% reduction in the vicinity of the summit. So, the shape of the volcano reduces drastically the vertical flux value measured near the summit and the characterization of internal sources of heat would mean having to take into account the exact shape.

## CONCLUSIONS

On both volcanoes the steady flux obtained fell within the range of uncertainty because of the unknown long-term climatic variations; contrary to the Etna case, the base fluxes are null or very small. Nevertheless, these values permit us to set several limits to the internal structure of the volcano, which is a very valuable result. More refinement was introduced by taking into account the effects of the general and local relief, but local relief and heat release linked to rain or sea water movement cannot be characterized with only one profile. As the study of conductive heat flux provides important information on volcanic areas (Sass and Morgan, 1988) it would be very interesting to develop this type of measurement and to have on the same edifice a net of temperature profiles. In such a case, as the long-term climatic variations would be identical at all the points, the map of flux differences would be totally free of this effect. The low cost of this method compared with flux determinations in drillholes, and the ease with which the profiles can be installed, even in difficult terrain, should also be emphasized.

*Acknowledgements*—The Argos monitoring equipment of Matthews and Hunter volcanoes was funded and installed by the geological and geophysical team (UR 1 F) of the Noumea O.R.S.T.O.M. Centre, as part of the MATHEMSIS and HUNTEMSIS projects. Data transmission was by the Argos system on N.O.A.A. satellites. Reception and processing of original data were performed by the Centre de Téléobservation Informatisée des Volcans, C.T.I.V. (C.R.G.—C.R.V., C.N.R.S.).

## REFERENCES

- Alfano, L. (1959) Introduction to the interpretation of resistivity measurements for complicated structural conditions. *Geophys. Prosp.* **8**, 311–366.
- Blot, C. (1976) Volcanisme et sismicité dans les arcs insulaires: prévision de ces phénomènes. *Géophys. ORSTOM, Paris* **13**.
- Carlsaw, M. S. and Jaeger, J. C. (1959) *Conduction of Heat in Solids*, 2nd edn. Clarendon Press, Oxford.
- Lardy, M. and Monzier, M. (1986) Rapport de mission sur l'installation de la station de volcano-sismologie sur le volcan Matthews. Rapport 3-86, ORSTOM-Nouméa, 54 pp.
- Lardy, M., Monzier, M. and Pambrun, C. (1988) Rapport de mission sur le volcan Hunter du 15 au 19 septembre 1989. Rapport 6-88, ORSTOM-Nouméa, 53 pp.
- Maillet, P., Monzier, M. and Lefevre, C. (1986) Petrology of Matthews and Hunter volcanoes, southern New Hebrides island arc (SW Pacific). *J. Volcanol. Geotherm. Res.* **30**, 1–27.
- Périsset, M. C. and Tabbagh, A. (1981) Calcul des variations transitoires lentes du flux de chaleur du sol en vue de l'interprétation des résultats obtenus en prospection thermique de subsurface. *La Météorologie* **24**, 39–46.
- Priam, R. (1964) Contribution à la connaissance du volcan de l'îlot Matthews (sud des Nouvelles Hébrides). *Bull. Volcanol.* **27**, 331–339.
- Sass, J. H. and Morgan, P. (1988) Conductive heat flux in VC1 and thermal regime of Valles caldera, Jemez Mountains, New Mexico. *J. geophys. Res.* **93**, 6027–6039.
- Tabbagh, A. (1985) A new apparatus for measuring thermal properties of soils and rocks *in-situ*. *I.E.E.E. Trans. Geosci. and Remote Sensing* **GE 23-6**, 896–900.
- Tabbagh, A. and Trézéguet, D. (1987) Determination of sensible heat flux in volcanic areas from ground temperature measurements along vertical profiles: the case study of Mount Etna. *J. geophys. Res.* **92**, 3635–3644.